Paper No.
9153

NACE INTERNATIONAL CORROSION 2017 Conference & Expo

Corrosion Inhibition of Pipeline Steels under Supercritical CO_2 Environment

Yoon-Seok Choi, Shokrollah Hassani, Thanh Nam Vu, Srdjan Nesic
Institute for Corrosion and Multiphase Technology,
Department of Chemical and Biomolecular Engineering, Ohio University
342 West State Street
Athens, OH 45701
USA

Ahmad Zaki B Abas, Azmi Mohammed Nor, Muhammad Firdaus Suhor
Petronas Research SDN. BHD, Selangor Darul Ehsan, Malaysia

ABSTRACT

It has been reported that aqueous corrosion rate of a carbon steel is very high under supercritical CO_2 condition. In the present study, the performance of imidazoline-based corrosion inhibitor was evaluated by examining environmental effects on the corrosion rate and corrosion behavior of materials. The tested parameters include material (X65, 1Cr steel and 3Cr steel), temperature, and concentration of inhibitors. The corrosion rates of samples were determined by electrochemical measurements. The surface morphology and the composition of the corrosion product layers were analyzed by using surface analytical techniques (SEM and EDS). Results showed that the addition of corrosion inhibitor decreased corrosion rate significantly from 90 mm/y to below 0.1 mm/y at supercritical CO_2 condition (12 MPa CO_2, 80^{o}C). Corrosion rates of carbon steels in the CO_2 saturated solution with the presence of inhibitor did not depend on the temperature. However, corrosion inhibitor performed better for the carbon steel than Cr containing steels in supercritical CO_2 environment.

Key words: Supercritical/liquid CO_2, CO_2 corrosion, carbon steel, corrosion inhibitor

INTRODUCTION

CO_2 corrosion of mild steel has been widely studied in the past 30 years and the field of corrosion in supercritical CO_2 has been of great interest recently. The published literature on supercritical CO_2 primarily addresses topics related to CO_2 sequestration and enhanced oil recovery that usually involve “dry” gases where water is only present at the ppm level.[1-3] However, due to the direct impact of the presence of formation water and high pressure CO_2 on the corrosion of pipeline steel, the corrosion rate of carbon steel at high CO_2 pressure (liquid and supercritical CO_2) without formation of protective $FeCO_3$ corrosion product layers is very high (≥ 20 mm/y).[4-8]

For corrosion control, sufficient drying (water removal) upstream of the pipeline is required in order to prevent breaking-out of free water and excessive corrosion rates.[9,10] However, it would be too costly to dry the gas stream in the field conditions. Since the corrosion mechanism of carbon steel is similar under both low CO_2 pressure and high CO_2 pressure,[11] employing corrosion inhibitors could be a promising strategy in order to control corrosion at high pressure CO_2 conditions.[12]

The performance of various inhibitors in the CO_2-saturated solution has been widely studied. Imidazoline-based inhibitors are the mostly used inhibitors in oil and gas field to control CO_2 corrosion. However, these studies were usually under low CO_2 pressure conditions related to oil and gas pipelines. For high CO_2 pressure conditions, publications are sparse which report on efficiencies of corrosion inhibitors in supercritical CO_2 systems.[12,13] Classic corrosion inhibitors such as imidazoline series, alkenylsuccinic acids and quaternary ammonium compounds were evaluated in supercritical CO_2 systems.[14] Although these chemicals did reduce the corrosion rate, none of them were fully effective. Corrosion inhibition of imidazoline-based inhibitors were evaluated at a high pressure and high temperature condition of 80 bar CO_2 and 70°C.[15] Insufficient inhibition from the imidazoline-type inhibitors caused localized corrosion, and the addition of thiosulfate had the capability to further reduce the corrosion rate compared with imidazoline inhibitor.

In the present study, the performance of imidazoline + thiosulfate corrosion inhibitor was evaluated by examining environmental effects on the corrosion rate and corrosion behavior of materials. The tested parameters include concentration of inhibitor, temperature and materials.

EXPERIMENTAL PROCEDURE

The materials tested in this work are as follow:

- UNS K03014 carbon steel, named CS
- UNS G41300-1Cr steel, named 1Cr
- UNS G41300-3Cr steel, named 3Cr

All materials were analyzed for chemical composition using Atomic Emission Spectroscopy (AES). Table 1 shows chemical compositions of the three materials used in the present study.

Table 1
Chemical compositions of materials used in the present study (wt.%, balance Fe).

	C	Cr	Mn	P	S	Si	Cu	Ni	Mo	Al
CS	0.065	0.05	1.54	0.013	0.001	0.25	0.04	0.04	0.007	0.041
1Cr	0.3	0.85	0.91	0.015	0.008	0.29	---	---	---	---
3Cr	0.08	3.43	0.54	0.006	0.003	0.3	0.16	0.06	0.32	---

The specimens for the corrosion tests were machined with two different geometries: cylindrical type with 5 cm^2 exposed area for electrochemical measurements, and rectangular type with a size of 1.27 cm × 1.27 cm × 0.254 cm for surface analysis. The specimens were ground up to 600-grit silicon carbide (SiC) paper, cleaned with isopropyl alcohol (*i*-C_3H_7OH) in an ultrasonic bath, and dried.

The corrosion experiments were carried out in a 7.5-liter autoclave (made of UNS N10276) which contained a working electrode, a high pressure/high temperature Ag/AgCl reference electrode and a platinum coated niobium counter electrode. A schematic of experimental setup is shown in Figure 1. The electrolyte was a deaerated 1 wt.% NaCl solution. In order to introduce flow, an impeller was used to stir the solution at a rotation speed of 1000 rpm (approximately corresponding to 1 m/s), stirring was maintained during the test.

In the present study, imidazoline derivative + thiosulfate corrosion inhibitor (CI) was selected to be evaluated under high pCO_2 environments based on our previous study, which showed that imidazoline + thiosulfate inhibitor represented better performance than imidazoline inhibitor in high pCO_2 environment and under stagnant condition.[15]

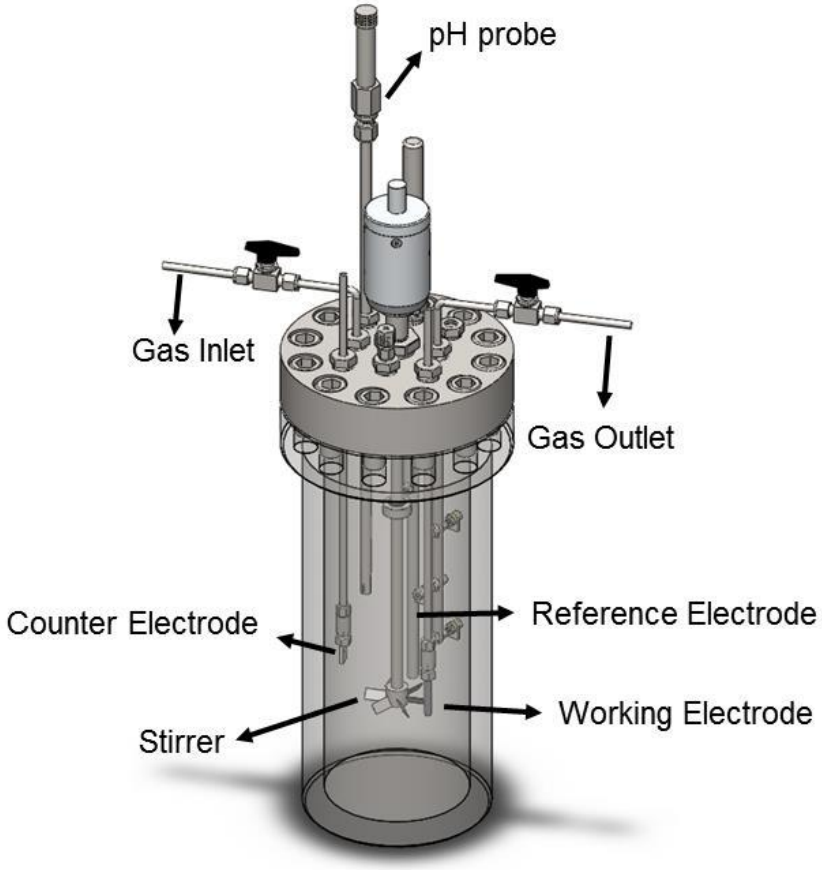

Figure 1: Schematic of autoclave system equipped for electrochemical measurements.

Table 2 shows the test conditions. During experiment, corrosion rates were monitored with LPR measurement made at regular time intervals. LPR measurements were performed in a range of ±5 mV with respect to the open circuit potential (OCP), and a scan rate of 0.125 mV/s. The polarization resistance (R_p) obtained from LPR measurement, was used to calculate the corrosion current density (i_{corr}) by using Eq. (1):

$$i_{corr} = \frac{B}{R_p} = \frac{\beta_a \times \beta_c}{2.3 \times R_p \times (\beta_a + \beta_c)} \quad (1)$$

where β_a is the anodic Tafel constant (40 mV/dec), β_c is the cathodic Tafel constant (120 mV/dec). Then, the i_{corr} was converted into corrosion rate using Eq. (2):

$$\text{Corrosion rate(mm/year)} = \frac{0.00327 \times i_{corr}(\mu A/cm^2) \times EW}{\text{density}(g/cm^3)} \quad (2)$$

where EW is the equivalent weight in grams and 0.00327 is a constant factor used for dimension and time conversion.

After the experiment, the specimen was taken to additional ex-situ analyses. The morphology and compositions of corrosion products were analyzed with SEM and EDS.

Table 2
Test matrix for corrosion testing

	Material	pCO_2 (bar)	Temperature (°C)	CI concentration (ppm_v)
Effect of concentration	CS	120	80	0
	CS	120	80	200
	CS	120	80	400
Effect of temperature	CS	120	25	400
	CS	120	80	400
Effect of material	CS	120	80	400
	1Cr	120	80	400
	3Cr	120	80	400

RESULTS AND DISCUSSION

Inhibition performance with different concentrations

Corrosion rates of CS at 120 bar and 80 °C in CO_2 saturated 1 wt.% NaCl solution with the presence of 0, 200, and 400 ppm of CI are shown in Figure 2. Without CI, the corrosion rate is about 90 mm/y at the beginning of the experiment (reminder: corrosion rate of uninhibited CS decreased after 15 h because of the change in solution chemistry and the formation of protective $FeCO_3$,[11,16,17] which will not happen in the field condition). With the presence of 200 ppm of CI, the initial corrosion rates were much lower than the uninhibited condition, however, the corrosion rate increased with time, indicating insufficient inhibition for the CI concentration of 200 ppm. With 400 ppm of CI, the corrosion rate decreased with time from 90 mm/y to below 0.1 mm/y which is the target of the inhibited corrosion rate.

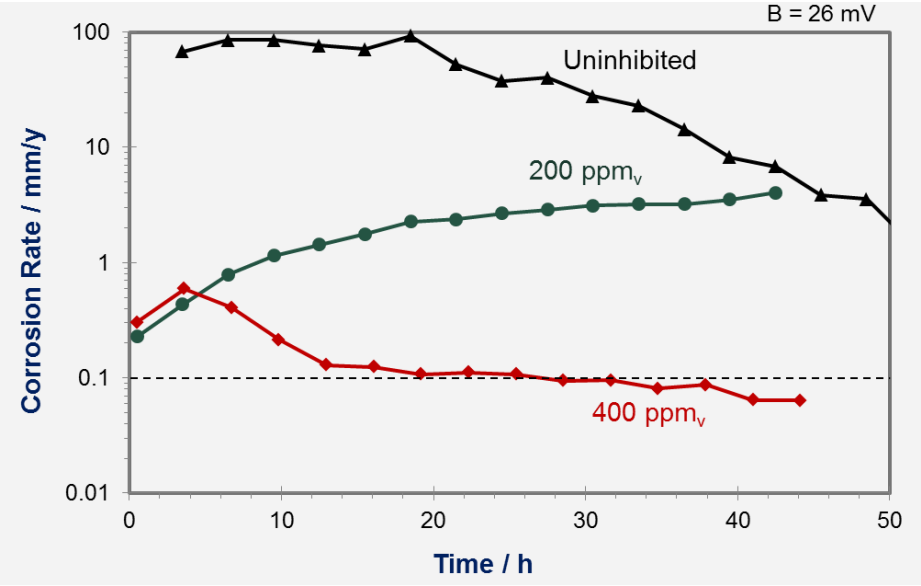

Figure 2: Corrosion rates of CS by LPR as a function of time with different concentrations of inhibitor in CO_2 saturated 1 wt.% NaCl under 120 bar and 80°C.

The results of surface analysis for samples after corrosion experiments with different concentrations of CI are shown in Figure 3. On the uninhibited sample surface, corrosion products were identified as $FeCO_3$ based on EDS analysis. On the sample surfaces with 200 ppm and 400 ppm of CI, there are corrosion products containing sulfur (Figure 3 (b) and (c)), possibly FeS, formed indirectly *via* disproportionation of the thiosulfate component in the inhibitor. There is stronger peak of S with 400 ppm of CI because of the doubled thiosulfate concentration for the 400 ppm experiment as to that conducted for 200 ppm of CI.

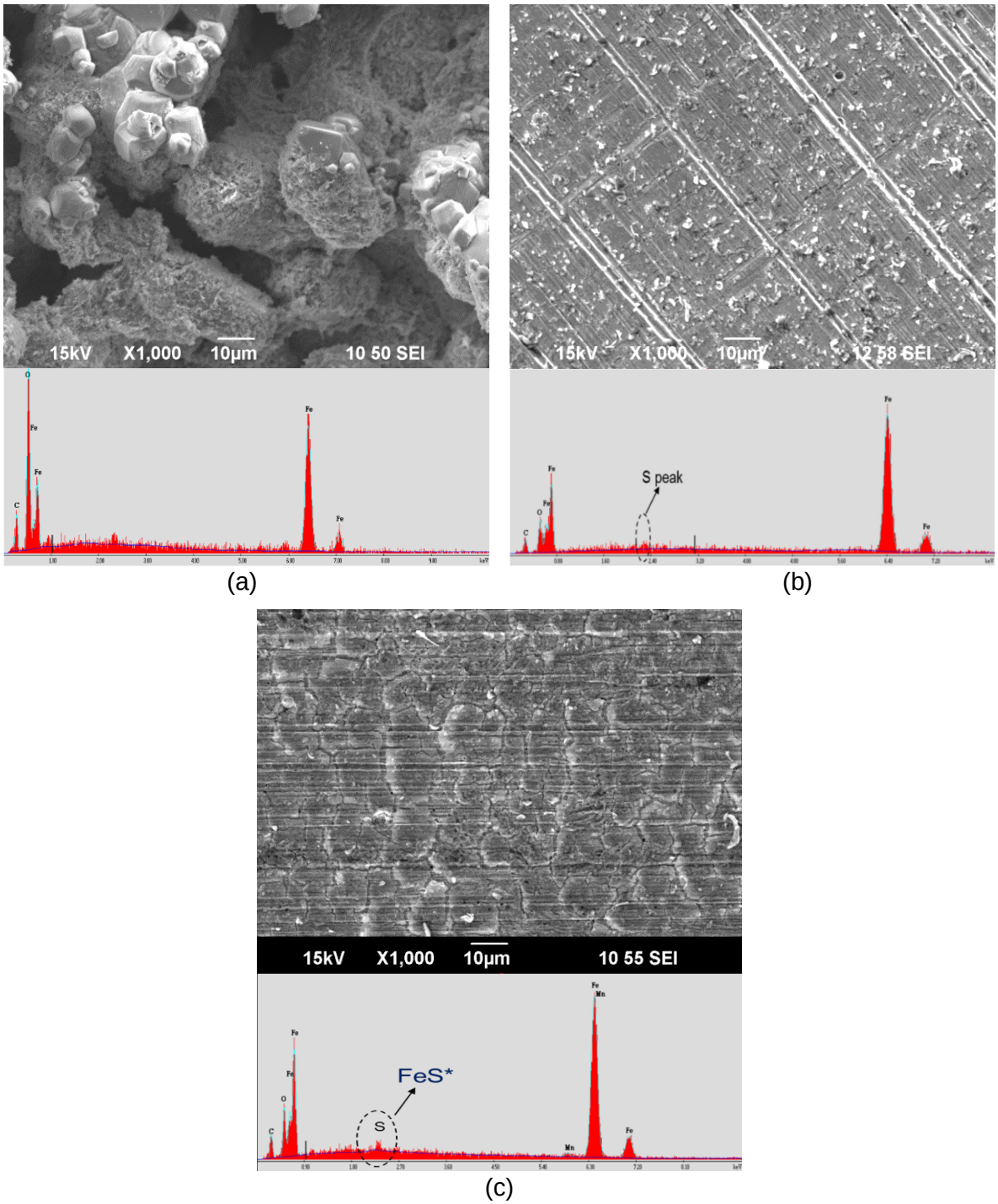

Figure 3: SEM images and EDS analysis of the sample surfaces after the inhibition tests with different CI concentrations at 120 bar and 80°C: (a) uninhibited, (b) 200 ppm CI, (c) 400 ppm CI.

Based on our understanding and the experimental results above, we proposed a hypothesis for the inhibition mechanism in the pure CO_2 environment. In this hypothesis, there are 2 steps:

- Step 1 (Figure 4 (a)): CO_2 saturated solution is an acidic media. In this media, thiosulfate (one of the main component of inhibitor) disproportionates to form sulfide which rapidly reacts with Fe to form FeS on the steel surface, as summarized by the following reaction:[18]

$$Fe + S_2O_3^{2-} + H_2O \rightarrow FeS + SO_4^{2-} + H_2 \quad (3)$$

- Step 2 (Figure 4 (b)): as soon as a thin layer of FeS was formed on the steel surface (this process is very fast based on the kinetics of the FeS formation reaction), an adsorption of the imidazoline derivative (the main component of the inhibitor) would happen. This adsorption may happen before the formation of FeS but, as mentioned above, the FeS formation is very fast so it would happen first. Moreover, the adsorption of the organic component on the steel surface covered by a thin FeS layer has been hypothesized to be stronger than on the bare steel surface.

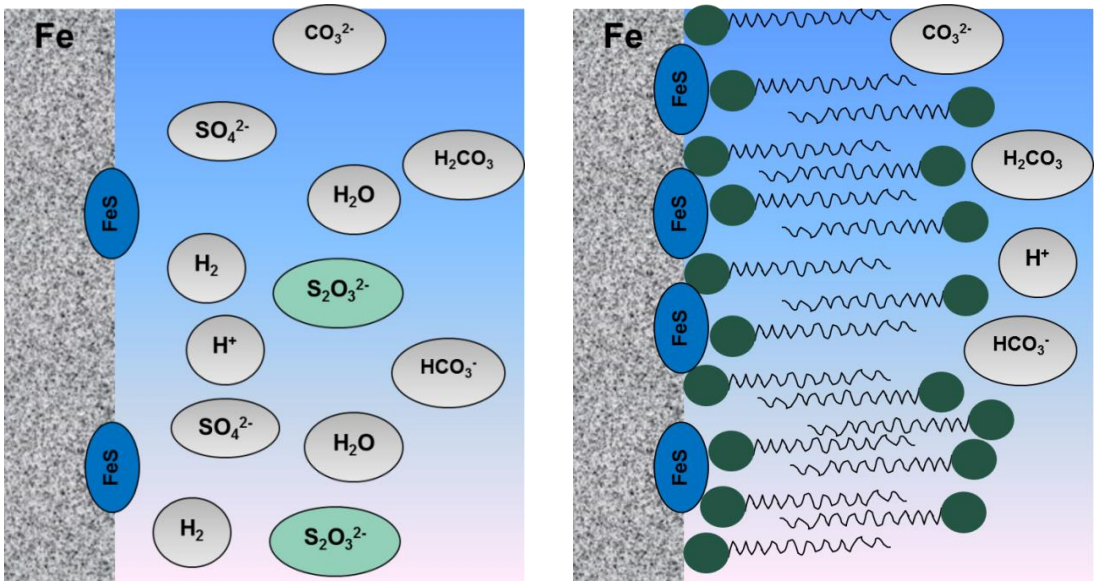

(a) (b)

Figure 4: Hypothesis for the inhibition mechanism in pure CO_2 environment: (a) Step 1- formation of FeS from thiosulfate, (b) Step 2- adsorption of the imidazoline derivative on FeS.

Inhibition performance at different temperatures

Figure 5 shows the variation of corrosion rate with time at different temperatures with 400 ppm of CI. It is interesting to note that corrosion rate of CS in the CO_2 saturated solution with the presence of 400 ppm of CI did not depend on the temperature.

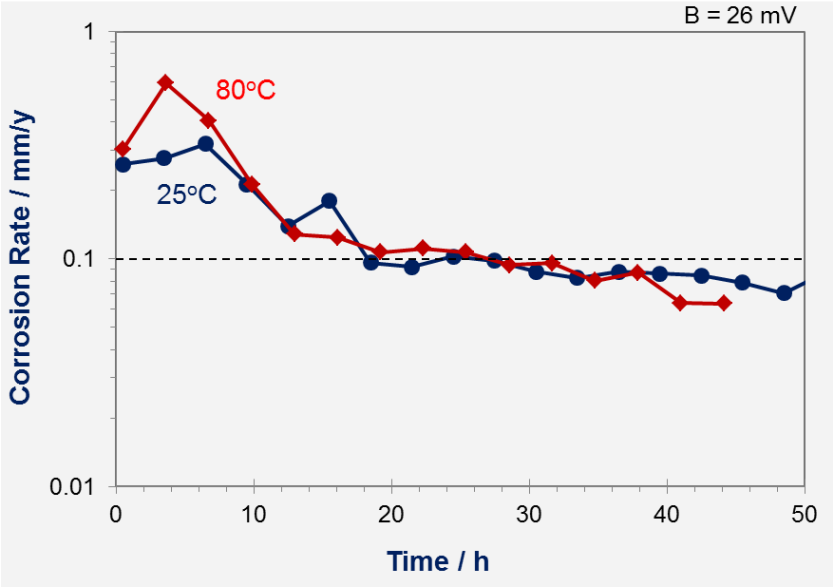

Figure 5: Corrosion rates of CS as a function of time in CO_2 saturated 1 wt.% NaCl solution at a pressure of 120 bar and temperatures of 25°C and 80°C with 400 ppm of Cl.

Results of surface analysis (Figure 6) indicated that there is more visible FeS on the sample at 80°C compared to the sample at 25°C. However, it doesn't affect the performance of inhibitor under this condition.

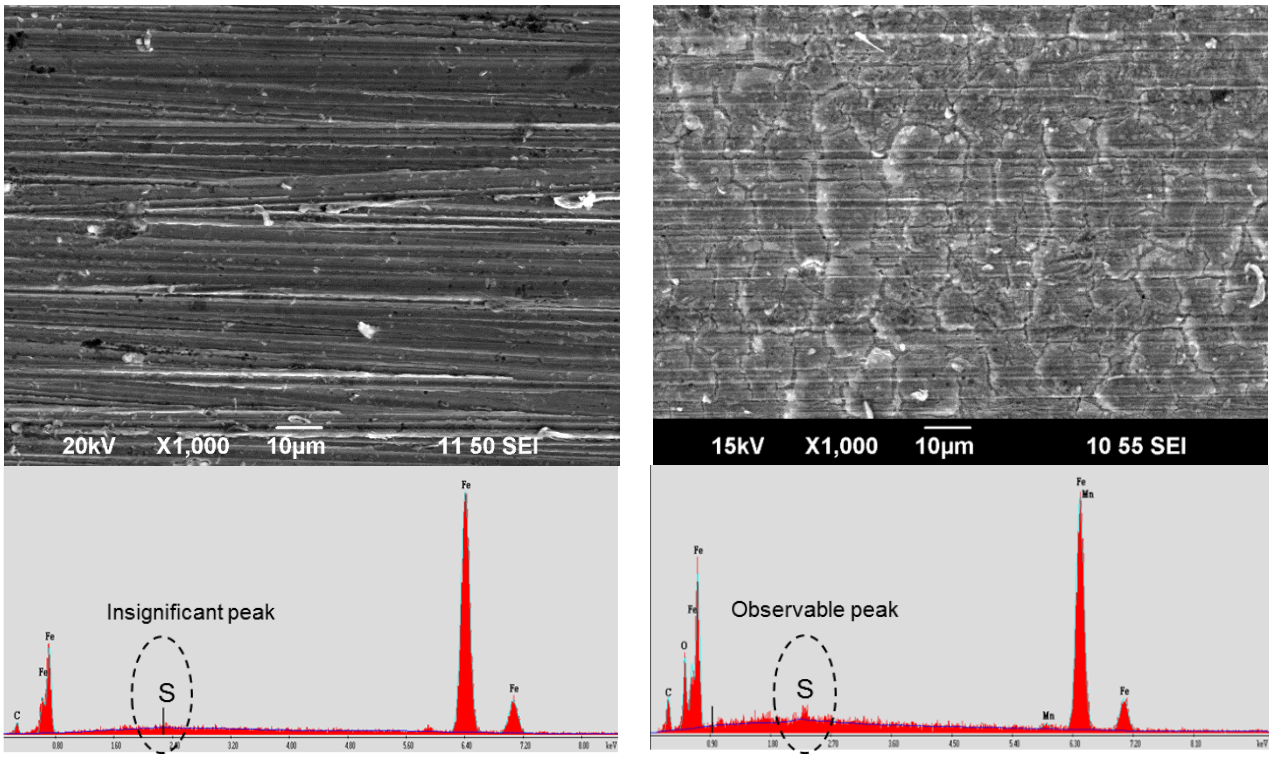

(a) (b)

Figure 6: SEM images and EDS spectra of the sample surface after the experiments with 400 ppm of Cl at 120 bar CO_2: (a) 25°C, (b) 80°C.

Inhibition performance with different materials

Figure 7 shows uninhibited corrosion behavior of different materials (CS, 1Cr, and 3Cr) at 120 bar and 80°C. 3Cr steel shows lower corrosion rate compared with CS and 1Cr steel. CS and 1Cr showed similar corrosion performance under this condition. CS and 1Cr showed a drop in corrosion rate after one or two days of experiment because experimental artifacts relating to changes in water chemistry of bulk solution and formation of $FeCO_3$. However, 3Cr steel showed lower corrosion rate from the beginning of experiments, which means that corrosion product layer immediately formed on the surface.

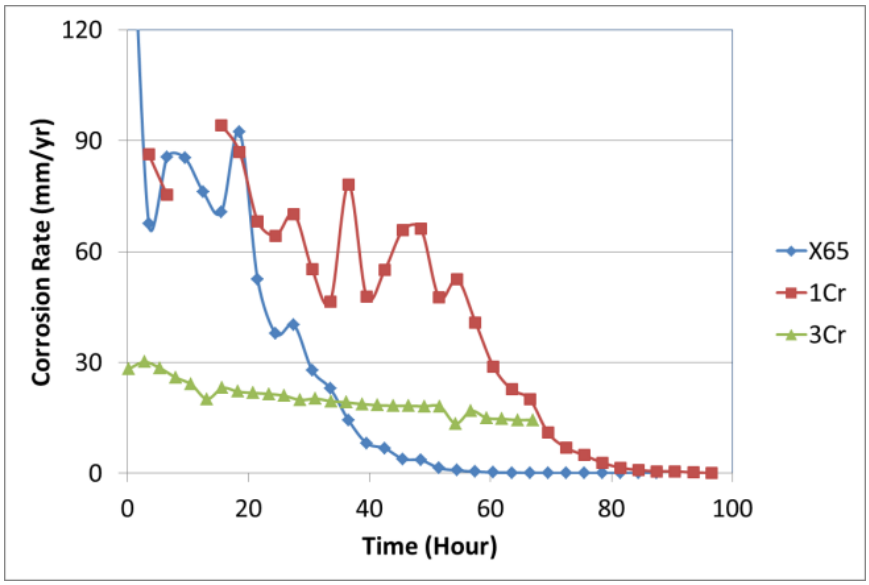

Figure 7: LPR corrosion rate data of CS, 1Cr, and 3Cr steels in CO_2 saturated 1 wt.% NaCl solution at 120 bar and 80°C.

Surface analysis (SEM, EDS, and XRD) was conducted to better explain performance of 3Cr steel at this condition (Figure 8 and Table 3). 3Cr steel forms a thick layer of corrosion products on the surface at 80°C which is not really protective because of the corrosion rate of 20 mm/y at the end of the experiment. This layer is Cr-rich, based on the EDS analysis shown in Table 3 but XRD only shows a weak peak of Fe. Therefore, this layer is amorphous as well as being chromium-rich.

Variation of corrosion rate of different materials at the same condition (120 bar and 80°C) with 400 ppm of CI is shown in Figure 9. Only corrosion rate of CS decreased to below 0.1 mm/y in the presence of 400 ppm of CI. This indicates that the inhibitor performed better for CS than Cr containing steels.

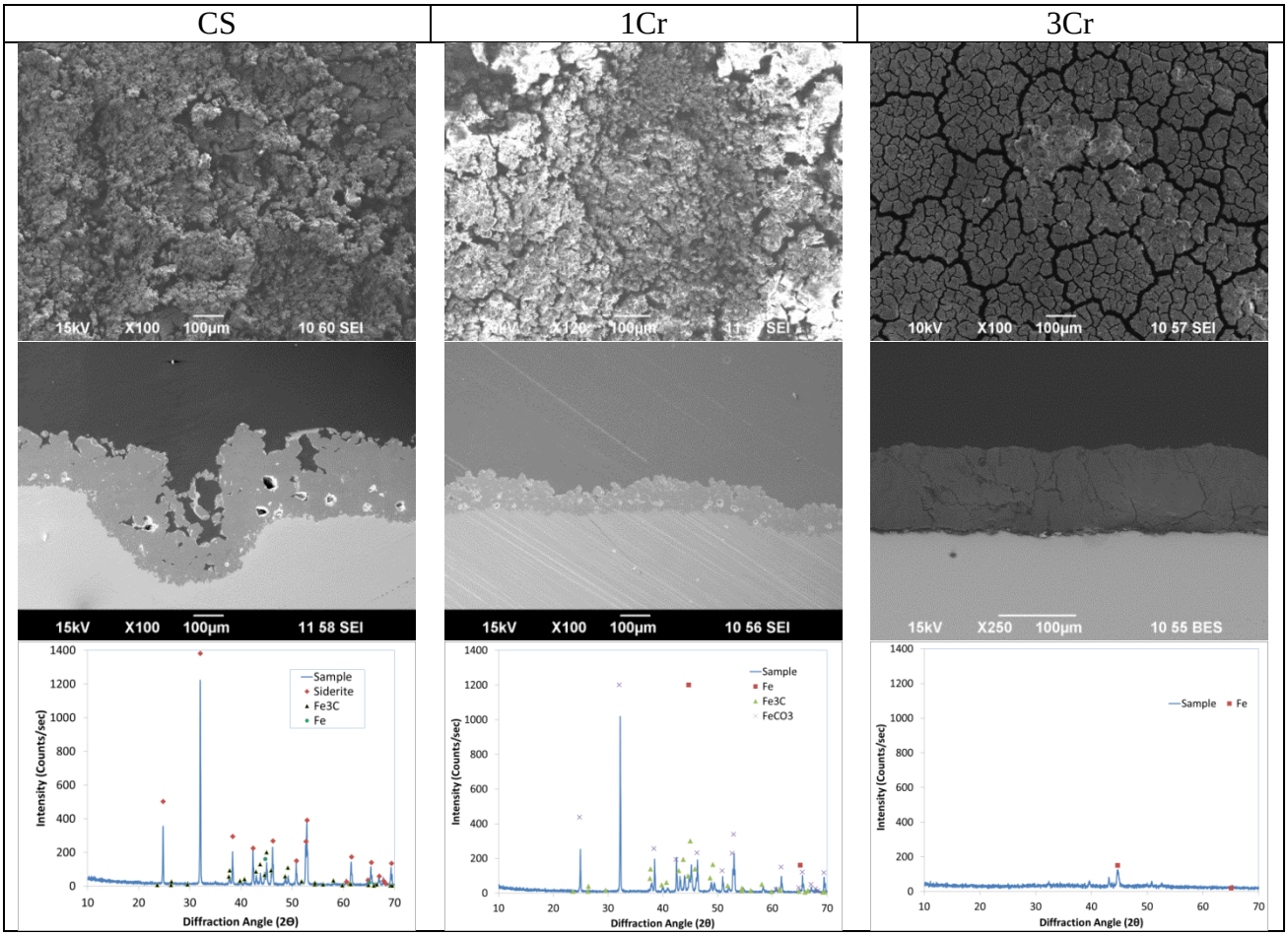

Figure 8: SEM and XRD surface analysis of CS, 1Cr and 3Cr steels after corrosion experiment at 120 bar and 80ºC in water phase saturated with CO_2.

Table 3
EDS surface analysis of CS, 1Cr and 3Cr steels after corrosion experiment at 120 bar and 80ºC in water phase saturated with CO_2

	CS	1Cr	3Cr
Element	Atomic %	Atomic %	Atomic %
C	31	42	66
O	35	28	17
Cr	0	1.3	13
Fe	25	29	2

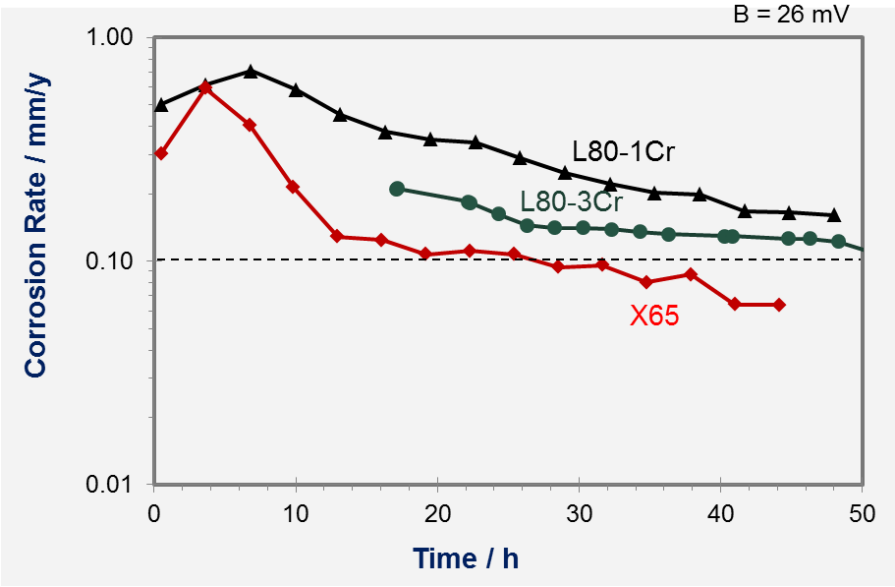

Figure 9: Corrosion rates of CS, 1Cr, and 3Cr as a function of time in CO_2 saturated 1 wt.% NaCl solution at 120 bar and 80°C with 400 ppm of Cl.

For better understanding as to why the corrosion performance of CS is worse than 1Cr and 3Cr materials in the uninhibited system but better than in the inhibited system, a surface analysis was performed on the 3 steels surface after the corrosion experiments (Figure 10). According to these results, all samples contain sulfur containing compounds (probably FeS) on the surface but the Cr enrichment was observed at the surface of 1Cr and 3Cr steels. This suggests that the formation of Cr rich layer on the surface could interrupt the formation of a coherent FeS layer.[19]

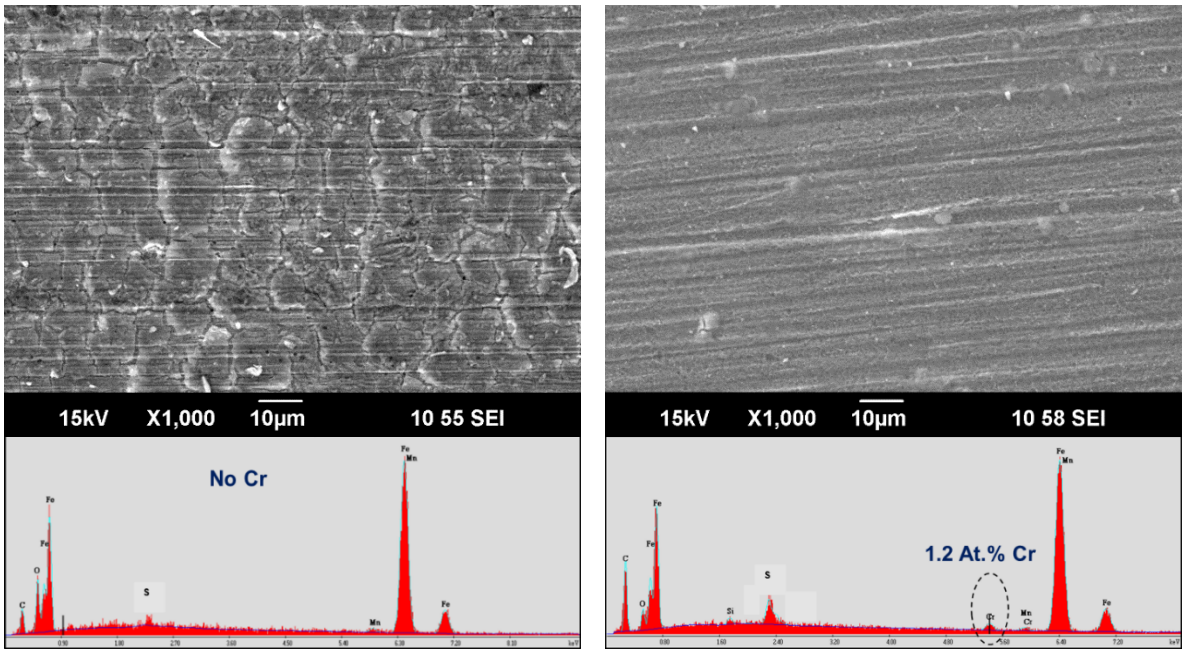

(a) (b)

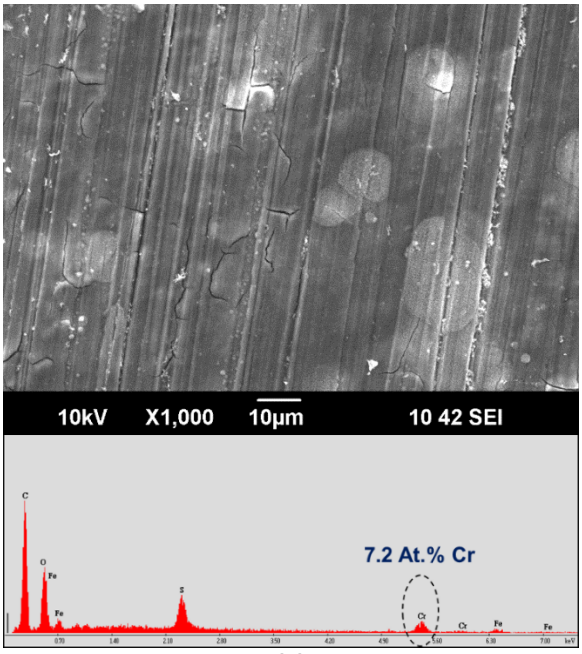

(c)

Figure 10: SEM images and EDS spectra of the sample surface after the experiments with 400 ppm CI at the condition of 120 bar and 80°C: (a) CS, (b) 1Cr, and (c) 3Cr.

CONCLUSIONS

The performance of imidazoline + thiosulfate CI was investigated by examining environmental effects such as concentration of inhibitor, temperature and materials at supercritical CO_2 condition. The following conclusions are drawn:

- At least 400 ppm of CI should be added in order to control the corrosion rate below 0.1 mm/y at 120 bar and 80°C condition.
- Temperature does not affect the inhibition performance in supercritical CO_2 environment.
- CI showed better protective performance on CS than 1Cr and 3Cr steels.

REFERENCES

1. Y.S. Choi, S. Nesic, D. Young, “Effect of Impurities on the Corrosion Behavior of CO_2 Transmission Pipeline Steel in Supercritical CO_2-Water Environments,” *Environmental Science and Technology* 44 (2010): p. 9233.
2. Y.S. Choi, S. Nesic, “Effect of Water Content on the Corrosion Behavior of Carbon Steel in Supercritical CO_2 Phase with Impurities,” CORROSION 2011, paper no. 11377 (Houston, TX: NACE, 2011).
3. S. Sim, F. Bocher, I.S. Cole, X.B. Chen, N. Birbilis, “Investigating the Effect of Water Content in Supercritical CO_2 as Relevant to the Corrosion of Carbon Capture and Storage Pipelines,” Corrosion 70 (2014): p. 185.
4. M.F. Mohamed, A. Mohammed Nor, M.F. Suhor, M. Singer, Y.S. Choi and S. Nesic, "Water Chemistry for Corrosion Prediction in High-pressure CO2 Environments," CORROSION 2011, paper no. 11375 (Houston, TX: NACE, 2011).

5. A. Mohammed Nor, M.F. Suhor, M.F. Mohamed, M. Singer and S. Nesic, "Corrosion of Carbon Steel in High CO2 Environment: Flow Effect," CORROSION 2011, paper no. 11245 (Houston, TX: NACE, 2011).
6. Y. Zhang, X. Pang, S. Qu, X. Li, K. Gao, "The Relationship Between Fracture Toughness of CO2 Corrosion Scale and Corrosion Rate of X65 Pipeline Steel Under Supercritical CO2 Condition," *International Journal of Greenhouse Gas Control* 5 (2011): p. 1643.
7. A. Mohammad Nor, M.F. Suhor, M.F. Mohamed, M. Singer, S. Nesic, "Corrosion of Carbon Steel in High CO_2 Containing Environments: the Effect of High Flow Rate," CORROSION 2012, paper no. 0001683 (Houston, TX: NACE, 2012).
8. Y.S. Choi, D. Young, S. Nesic, L.G.S. Gray, "Wellbore Integrity and Corrosion of Carbon Steel in CO_2 Geologic Storage Environments: A Literature Review," *International Journal of Greenhouse Gas Control* 16S (2013): p. S70.
9. M. Seiersten, K.O. Kongshaug, "Materials Selection for Capture, Compression, Transport and Injection of CO_2", in Carbon Dioxide Capture for Storage in Deep Geologic Formations, Vol. 2, D.C. Thomas and S.M. Benson Eds. (Elsevier Ltd. 2005), pp. 937
10. G. Heggum, T. Weydahl, M. Molnvik, and A. Austegaard, "CO_2 condition and transportation", in Carbon Dioxide Capture for Storage in Deep Geologic Formations, Vol 2, D.C. Thomas and S.M. Benson Eds. (Elsevier Ltd. 2005), pp. 925
11. Y. Zhang, X. Pang, S. Qu, X. Li, K. Gao, "Discussion of the CO2 Corrosion Mechanism Between Low Partial Pressure and Supercritical Condition," *Corrosion Science* 59 (2012): p. 186.
12. S. Sim, I. S. Cole, Y. S. Choi, N. Birbilis, "A Review of the Protection Strategies against Internal Corrosion for the Safe Transport of Supercritical CO_2 via Steel Pipelines for CCS Purposes," *International Journal of Greenhouse Gas Control* 29 (2014): p. 185.
13. S. Turgoose, G. John, M. Flynn, "Corrosion Inhibition in Supercritical Carbon Dioxide Systems Containing Water," CORROSION 2014, paper no. 4048 (Houston, TX: NACE, 2014).
14. Y. Zhang, K. Gao, G. Schmitt, "Inhibition of Steel Corrosion under Aqueous Supercritical CO2 Conditions," CORROSION 2011, paper no. 11379 (Houston, TX: NACE, 2011).
15. Mohd Farid Mohamed, "Water Chemistry and Corrosion Inhibition in High Pressure CO_2 Corrosion of Mild Steel," Master thesis, (Ohio University, 2015).
16. M.F. Suhor, M.F. Mohamed, A. Mohammad Nor, M. Singer, S. Nesic, "Corrosion of Mild Steel in High CO_2 Environment: Effect of the $FeCO_3$ Layer," CORROSION 2012, paper no. 0001434 (Houston, TX: NACE, 2012).
17. Y.S. Choi, F. Farelas, S. Nesic, A.A.O. Magalhães, C. de Azevedo Andrade, "Corrosion Behavior of Deep Water Oil Production Tubing Material under Supercritical CO_2 Environment: Part 1—Effect of Pressure and Temperature," *Corrosion* 70 (2014): p. 38.
18. M. Kappes, G. S. Frankel, N. Sridhar and R. M. Carranza, "Corrosion Behavior of Carbon Steel in Acidified, Thiosulfate-Containing Brines," *Corrosion* 68 (2012): p. 872.
19. L. D. Paolinelli, T. Pérez, S. N. Simison, "The Incidence of Chromium-Rich Corrosion Products on the Efficiency of an Imidazoline-Based Inhibitor used for CO_2 Corrosion Prevention," *Materials Chemistry and Physics* 126 (2011): 938.